Development of a ship eco-driving prototype for inland waterways

F. Linde[1], N. Huybrechts[2], A. Ouahsine[3], and P. Sergent[4]

ABSTRACT

The aim of this article is to develop a speed optimization software for inland navigation allowing to reduce fuel consumption by specifying a recommended sailing speed for each leg of the travel. For a given route, the water depth and currents are predicted with a 2D hydraulic model (Telemac 2D). Each leg of the route are then assigned a mean water depth and current velocity and resistance curves are obtained with a ship resistance model, based on a metamodel approximating CFD calculations or experimental results for ship resistance [Linde et al., 2015]. The fuel consumption is estimated with the model developed by Hidouche & Guitteny [2015]. The gradient projection algorithm [Rosen, 1960] is used to minimize the global fuel consumption for the itinerary. This model is used to simulate a real case: the itinerary of a 135 m self-propelled ship on river Seine, between Chatou and Poses (153 km). The optimized fuel consumption is compared with the non optimized fuel consumption, based on AIS speed data gathered on this itinerary. Different river discharges (low, medium and high) and sailing directions (upstream and downstream) are studied. The effects of the ship trajectory and travel duration on fuel consumption are also investigated.

1. INTRODUCTION

Inland waterway offers many advantages compared to roads and railways. The accident probability is very low and their cost in economic and human term is significantly reduced compared to the other means of goods transport. Inland waterways have little or no congestion and delay in goods delivery is hence reduced. A pushed barge with a load of 2 000 tons carries the equivalent of 50 railway cars at 40 tons each or 80 trucks at 25 tons each and therefore the carrying capacity per transport unit is very high. Moreover as pointed out by several studies [Rohacs and Simongati, 2007; Federal German Water and Shipping Administration, 2007; Agence de l'Environnement et de la Maitrise de l'Energie, 2006], inland waterway transport features as the most environmentally friendly mode. Making inland waterway transport more efficient and more sustainable is also one of the goals promoted by the European Commission through the NAIADES II package.

Even if the French waterway system is the longest in European Union with approximately 8800 km of navigable rivers and canals, French inland waterway transport (IWT) sector is lagging behind its European neighbors. IWT in France only represents 6% of all goods transport against 12% for Germany, 16% for Belgium and 33% for the Netherlands. One of the actions led by the French authorities to promote IWT is the construction of Seine-Nord Europe Canal. This new channel is expected to replace the existing Canal du Nord of limited capacity (barges of 250 to 650 tonnes) to form a major high capacity transport corridor for barges and push-tows up to 4400 tonnes, from Le Havre to Dunkirk, Benelux and the Rhine. Beside this hydraulic work, significant research efforts must still be conducted in order to improve inland vessel fuel efficiency. Indeed, inland navigation faces several challenges such as over-aging fleet, increasing fuel prices, climate change, and stronger environmental regulations regarding air emissions.

_____
[1] PhD, DTecEMF, CEREMA, 134 rue de Beauvais - CS 60039, 60280 Margny Lès Compiègne, France, florian.linde@cerema.fr

[2] Researcher, Sorbonne Universités, Université de Technologie de Compiègne, CNRS, Laboratoire Roberval UMR 7337, Centre de Recherches de Royallieu, CS 60319, 60203 Compiègne Cedex, France.

[3] Professor, Sorbonne Universités, Université de Technologie de Compiègne, CNRS, Laboratoire Roberval UMR 7337, Centre de Recherches de Royallieu, CS 60319, 60203 Compiègne Cedex, France.

[4] Researcher, DTecEMF, CEREMA, 134 rue de Beauvais - CS 60039, 60280 Margny Lès Compiègne, France.

The Lower Seine River is one of the main fluvial corridors in France. This river welcomes different ports at Le Havre, Rouen, and Gennevillier just downstream Paris. Each day, several vessels are travelling between Le Havre and Gennevillier. In order to reduce the fuel consumption and gas emission, it is proposed here to build a fluvial eco-driving prototype. Up to now, this prototype called "EcoNav" has been applied only on the Lower Seine River for one vessel type. The selected vessel type corresponds to a 135 m long and 11.4 m wide self-propelled vessel. This vessel type has been selected as their number is expected to increase in the next years and other projects are currently led on it as experimental tests or maneuverability studies. On board fuel monitoring is also planned in a near future for such vessel.

In the current paper, different solutions to reduce fuel consumption are first reminded and a literature review is proposed. The methodology inside the Econav model is then described. EcoNav model combines different sub-models as a 2D hydraulic model, a ship resistance model, a fuel consumption model and a nonlinear optimization algorithm to find optimal speed profile. Econav is used to simulate a real case: the itinerary of the self-propelled ship Oural (from Compagnie Fluviale de Transport) on river Seine, between Chatou and Poses (153 km). The optimized fuel consumption is compared with the non optimized fuel consumption, based on AIS speed profile retrieved on this itinerary. The effects of the ship trajectory and travel duration on fuel consumption are finally investigated.

2. **Existing solutions for inland ship fuel consumption reduction**

The average age of inland ships in Europe is above 40 years and a significant proportion of the current fleet is over-aged. Replacing the older ships with new units will take decades and therefore improving the economic and environmental performance of existing ships (retrofitting) is also necessary. The European FP7 project MoVe IT! [MoVe IT! FP7 European project, 2012] and the Danube Carpathian Programme [Radojfici´c, 2009] reviewed the existing solutions for improving the economic and environmental performance of existing or new inland vessels. These solutions can mainly be categorized into four main groups: (1) improvement in hull resistance; (2) improvement in propulsion and transmission efficiency; (3) improvement in propulsion plant; and (4) improvement of ship utilization (navigation).Those four categories are outlined in Figure 1 with solution examples.
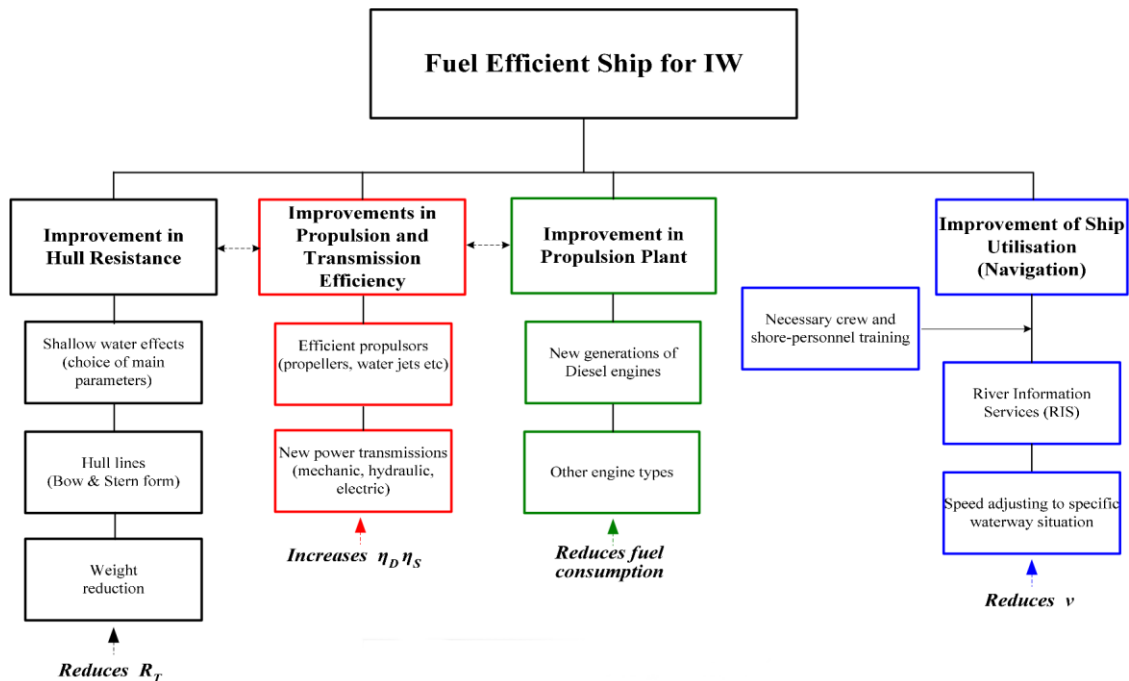

Figure 1: Main categories of retrofitting solutions [Radojčić, 2009]

2.1 Improvement in hull resistance

Decreasing hull resistance allows to reduce the forces opposing the movement of the ship and therefore leads to fuel consumption savings. Hull resistance can be decreased by adapting the hull shape to minimize resistance in shallow water. Hull shape optimization has mainly be focused on the design of efficient bow and stern regions [Rotteveel et al., 2014] which mostly contribute to wave and viscous pressure resistance. Zoelner [2003] showed that contemporary ships with improved designs have up to 50 % lower resistance than inland ships from a few decades ago. Another way to reduce hull resistance is to make the ship hull lighter. The materials used for inland ship construction is almost exclusively steel because of its durability. However, the use of lightweight materials and structural arrangements (such as reinforced composites materials or sandwich structure) for shipbuilding [Noury et al., 2002] could lead to significant fuel consumption reduction. For instance, Jastrzebski et al. [2003] reported a structural weight saving of 40 % if steel sandwich panels would be used for the construction of a small barge of 32.5 m. Solutions intending to decrease the frictional resistance of the hull have also been studied. For instance, the frictional drag can be reduced by using air as a lubricant with techniques such as injecting air bubbles in the boundary layer, using air films along the bottom plating or air cavities in the ship's bottom [Foeth, 2008]. It is also possible to reduce the ship resistance by applying special coatings with anti-fouling properties allowing to reduce water friction [Stenzel et al., 2011].

2.2 Improvement in propulsion and transmission efficiency

Many existing inland ships are built with conventional propellers whose efficiency often reach 70 % in maritime navigation but can be as low as 20-40 % when used in restricted waterways [Georgakaki and Sorenson, 2004]. Replacing those conventional propellers with one more suited to inland navigation could lead to significant fuel consumption reduction. For example, Geerts et al. [2010] reported that the three blade propeller of the Campine-Barge 'Prima' was replaced with a five-blade propeller which led to a speed gain of 1 km/h for the same fuel consumption. Many examples of innovative propellers more suited to inland navigation exist [MoVe IT! FP7 European project, 2012]: ducted propeller with a non-rotating nozzle which deliver greater thrust; adjustable tunnel preventing the income of air at low draft; pre swirl stator redirecting the flow before it enters the propeller disc; skew or contra-rotating propellers.

2.3 Improvement in propulsion plant

Currently, diesel engines are the most common types of engines used for inland ships. However, those engines are often marinized general application diesel engines or truck engines. Those engines are also usually much older than those used for road transport and belong to previous technological generation (inland ship engine have a lifetime of 20 years against 5 years for truck engines). Therefore, inland ships emit non-negligible quantities of carbon dioxide (CO_2), sulphur-oxides (Sox), nitrogen-oxides (NOx) and particulate matter (PM). With increased environmental legislation on transport emissions, inland shipping will need to reduce its greenhouse gas emissions and can benefit from the use of alternative fuels or im proved diesel engines. Possible solutions for improvement in propulsions plants include [MoVe IT! FP7 European project, 2012]:

• diesel electric propulsion where diesel powered generators provide electrical power used to propel the ship;

• hybrid propulsion using more than one power source to propel the ship (diesel generator with batteries for instance);

• natural gas engines using liquefied natural gas (LNG) instead of ordinary fuel;

• multi (truck) diesel electric using several truck diesel engines as generators in a diesel electric propulsion;

• fuel cell converting the chemical energy of a fuel (hydrogen or natural gas for instance) into direct current power.

2.4   Improvement of ship utilization (navigation)

Improvement in ship operations, aiming to reduce and/or adjust the ship speed during a travel can also lead to fuel consumption reduction. For instance, a traffic control system indicating the availability of locks and quays to ship operators could help them adjust their speed during the travel in order to minimize fuel consumption while ensuring to respect their ETA. River information services (RIS) offering possibilities for voyage planning, tracking and tracing through rapid electronic data transfer (in real-time) can contribute to a safe and efficient transport process and lead to a reduction of fuel consumption. Replacing the smaller fleet units or in creasing the ship main dimensions can help to lower the emissions per tonnekm. Prediction of the water depth on the ship route can help to adjust the ship speed in the shallow water zones. Applying slow steaming, which consist in sailing at a reduced speed, can also lead to consumption reduction.

2.5   Slow steaming and speed optimization

A ship sailing at a reduced speed will emit less greenhouse gas and consume less fuel. This practice, also known as slow steaming, is already used in many maritime commercial ship sectors such as tankers, bulk carriers and containerships, but rarely applied for inland navigation. A basic application of slow steaming consists in sailing at a speed lower than the vessel's design speed. More evolved slow steaming practices involve speed optimization algorithm taking account of several factors (weather forecast, current, trim, draft and water depth) [Psaraftis and Kontovas, 2014]. Some industrial products such as Eniram speed[1] already exist and are frequently used for maritime navigation. However, to the knowledge of the author, no such products exist or are used for inland navigation. A prototype version of the EconomyPlanner is currently developed and tested within the framework of the FP7 Eu project MoVeIT! (Bons et al., 2014). The aim of the EconomyPlanner is to generate a real time local water depth map through cooperative depth measurements and determine the optimal track and vessel speed respecting ETA (expected time of arrival) conditions for a given itinerary in order to reduce fuel consumption. The optimization of the fuel consumption is carried out by a module named Virtual Ship and developed by MARIN (Maritime Research Institute Netherlands). The power and resistance calculations are based on formulas derived from regression analysis on model experiments carried out at MARIN and sea trials. Corrections of shallow water effect are made based on Schlichting (1934) and Landweber (1939) methods.

3. Model development

Through an optimization algorithm minimizing the fuel consumption, the EcoNav model looks for the best speed profile for a given itinerary with operating conditions and under specified constraints. The constraint used in the optimization process is the maximum travel duration T_{max}. The model for fuel consumption FC_T computes the fuel specific consumption corresponding to the thrust input necessary to counteract the ship resistance. This ship resistance represents the hydrodynamic force R_T opposing the ship movement for given conditions (ship's load, channel geometry conditions, ship's speed, and current velocity). Finally, the operating conditions are defined by the parameters describing the hydrodynamics conditions in which the ship will sail on the itinerary. These conditions are the channel width W, the water depth H and the current velocity U. The last two quantities are predicted by using a 2D hydrodynamic model (Telemac2D V7P0). Figure 2 illustrates the working principle of EcoNav.
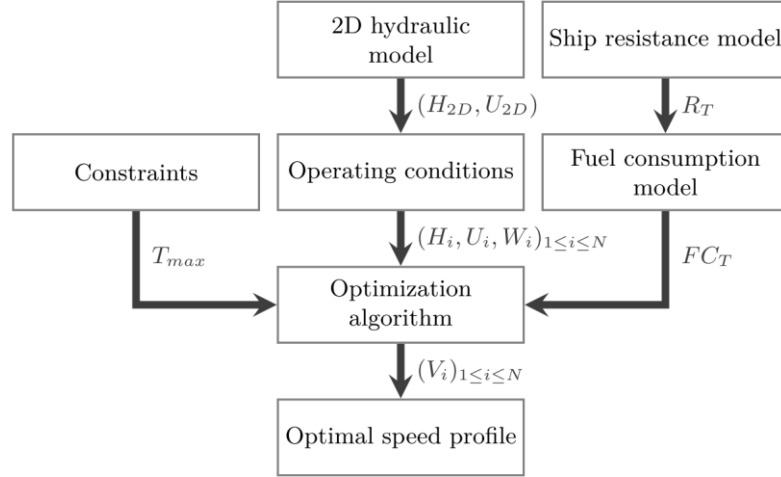
Figure 2: EcoNav flowchart

Each module is described in the following sections.

3.1   Ship resistance model

The fuel consumption of the ship is directly linked to the effective towing power $P_E = R_T \times V$ required to move the ship at a constant speed V. The ship resistance R_T can be evaluated in different ways: empirical formulae, CFD (Computational Fluid Dynamics) model or experimental data. As pointed out by Linde et al [2017], empirical formulae are not efficient in restricted waterways especially for narrow section. It is thus proposed to rather work with a surrogate model built from sampled data. The surrogate model could be fed with CFD results, experimental data or a combination of both of them. Here for the studied vessel, several experimental data have been conducted at Anast Lab from Liege University Belgium [Linde et al 2017]. It is thus chosen to only feed the surrogate model with these experimental data.

In order to avoid repeated use of computationally expensive simulations or costly experiments, surrogate models are often used to provide rapid approximations of more expensive models. These models are used in the engineering community for a wide range of application (Koziel and Leifsson, 2013).

The surrogate modelling approach approximates the simulation or experimental data $f_p(x)$ with the surrogate model output $\widehat{f}_p(x)$:

$$f_p(x) = \widehat{f}_p(x) + \varepsilon(x) \tag{1}$$

where x is the coordinate vector where the function is evaluated and $\varepsilon(x)$ is the approximation error.

The governing parameters used for this surrogate model are the water depth H to ships draught T ratio H/T (quantifying the water depth restriction); the channel width W to ships breadth B ratio W/B (characterizing the channel width restriction) and the vessels speed V. It is worth mentioning that those parameters are independent and characterize the three main factors who have an effect on ship resistance in restricted waterway. As a result, the ship total resistance RT is expressed as follows:

$$R_T = f\left(V, \frac{H}{T}, \frac{W}{B}\right) = f(X) = \widehat{R_T} + \epsilon \tag{2}$$

where $X = (V, \frac{H}{T}, \frac{W}{B})$ is the coordinate vector and $\widehat{R_T}$ is the approximation function of R_T given by the surrogate model.

Popular surrogate model techniques (Queipo et al. 2005, Forrester and Keane 2009; Simpson et al. 2008) include ordinary least square (LSM), moving least square (MLS), Kriging, support vector regression (SVR) and radial basis functions (RBF). Different approaches have been tested and their accuracies have been compared via the mean square error (MSE):

$$MSE = \frac{1}{n}\sum_{i=1}^{n}\left(R_{Ti} - \hat{R}_{Ti}\right)^2 \tag{3}$$

Where $\left(\hat{R}_{Ti} = \hat{R}_T(X_i)\right)_{i=1..n}$ are the n predictions of the n observed data points $\left(R_{Ti} = R_T(X_i)\right)_{i=1..n}$.

3.2   Ship fuel consumption model

To evaluate fuel consumption, it is necessary to calculate the break power P_B delivered by the main engine to move the ship at a speed V. However, this power is greater than the effective towing power $P_E = R_T \times V$ because of the various energy losses occurring in the ship propulsion. The main components of ship propulsion are:

- a prime mover engine transforming an energy source into rotational mechanical energy;

- a reduction gear reducing the high rotation speed of the engine;

- a main shaft supported and held in alignment by bearings and transmitting the rotational mechanical energy from the reduction gear to the propeller;

- a propeller converting rotational motion into thrust by imparting velocity to a column of water and moving it in the opposite direction of the ship movement.

The energy loss occurring between each energy transformation is quantified through efficiencies:

- the hull efficiency $\eta_H = P_E/P_T$ is the ratio between the effective power P_E and the thrust power P_T delivered by the propeller to the water,

- the propeller efficiency $\eta_B = P_T/P_B$ is the ratio between the thrust power P_T and the power delivered to the propeller P_B;

- the shaft efficiency $\eta_S = P_D/P_B$ is the ratio between the power P_D delivered to the propeller and the brake power P_B delivered by the main engine.

The global propulsion efficiency η_G is defined as the product of the three efficiencies described above:

$$\eta_G = \eta_H \times \eta_B \times \eta_S \tag{4}$$

Figure 3 illustrates the performance quantification of a typical ship propulsion.
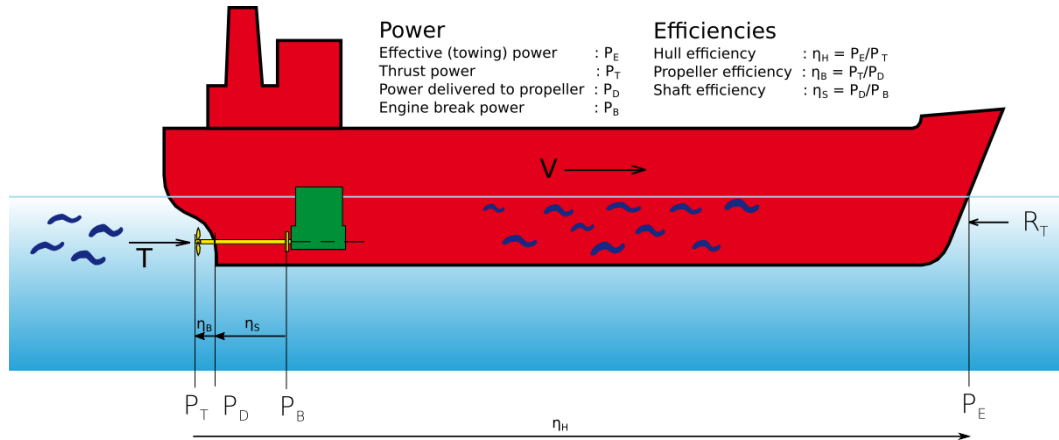

Figure 3: Performance of a typical ship propulsion [adapted from MAN, 2011]

The link between the breakpower P_B delivered by the main engine and the effective power P_E can be written as:

$$P_B = \frac{1}{\eta_H \times \eta_B \times \eta_S} P_E = \frac{1}{\eta_G} P_E \tag{5}$$

From the engine break power P_B [kW], the fuel consumption rate $\dot{m}_f$ [kg/h] is calculated through the specific fuel consumption SFC [kg/kW/h] (Eq.)

$$SFC = \frac{\dot{m}_f}{P_B} \tag{6}$$

The global propulsion efficiency η_G is taken equal to 0.5 which corresponds to an average value observed for inland vessels [Hidouche et al., 2015]. However, this estimation could be more accurate if each performance ratio is detailed, especially the propeller efficiency, but this implementation needs other parameters (propeller characteristics, hull shape,...) .

The specific fuel consumption model is based on a regression analysis of specific fuel consumption curves against power ratio (P_B/P_{max}). The specific fuel consumption data from recent and representative engine were collected from the manufacturers (mainly Cummins, MAN, Caterpillar and Wartsila). Furthermore, the declination of the model by engines power class and the split of the model in two zones of regression (power regression for zone 1 and polynomial regression for zone 2) provide a better accuracy to this model.

Figure 4 illustrates the regression analysis and Table 1 summarizes the equations of the ship consumption model and the error range.
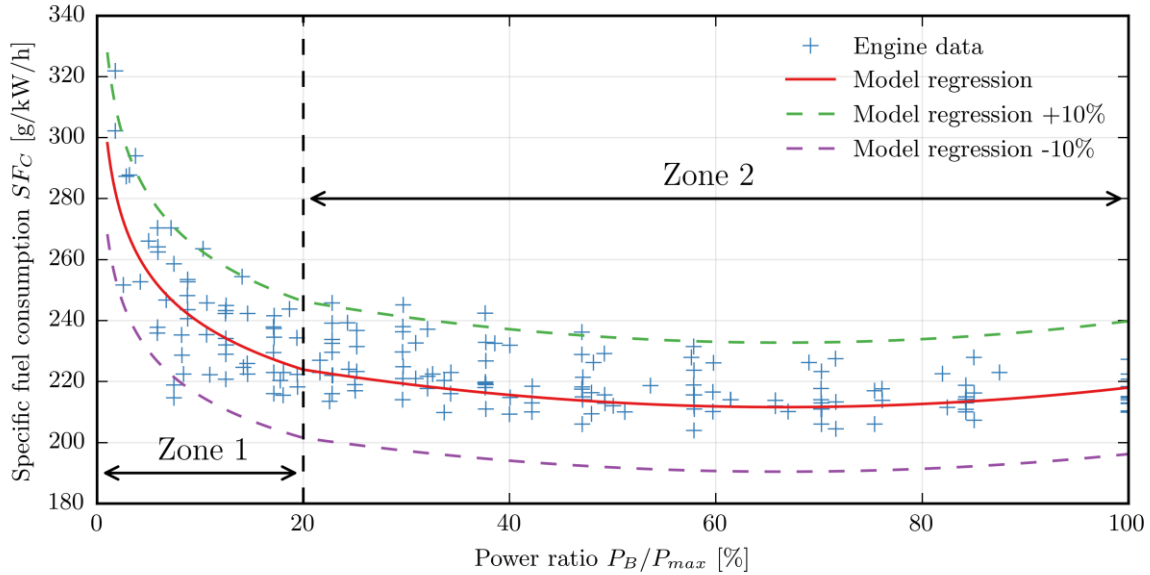

Figure 4: Specific fuel consumption model for 1000kW-2000kW range; model curve and engine data (adapted from Hidouche and Guitteny [2015])

$\mathbf{P_{max}}$ [kW]	$\mathbf{X = P_B/P_{max}}$ [%]	$\mathbf{SFC = f(X)}$ [g/kW/h]	**Error** [%]
100-300	$0-20$	$398.89(X)^{-0.1987} + 8.945$	10
	$20-100$	$242.51 - 0.810(X) + 0.0065(X)^2$	7
300-500	$0-20$	$342.077(X)^{-0.1361}$	10
	$20-100$	$237.84 - 0.5957(X) + 0.0040(X)^2$	7
500-1000	$0-20$	$327.708(X)^{-0.1262} + 1.984$	15
	$20-100$	$230.192 - 0.4496(X) + 0.0033(X)^2$	10
1000-2000	$0-20$	$296.346(X)^{-0.0963} - 1.06$	10
	$20-100$	$236.786 - 0.7577(X) + 0.0064(X)^2$	10
2000-10000	$0-30$	$265.583(X)^{-0.0570} - 1.743$	7
	$30-100$	$240.204 - 0.9639(X) + 0.0064(X)^2$	5
> 10000	$0-30$	$218.92(X)^{-0.0570} - 1.4368$	-
	$30-100$	$198 - 0.7945(X) + 0.0053(X)^2$	5

Table 1: Specific fuel consumption model equations and errors

3.3   2D hydraulic model

Flow characteristics must be provided along the vessel journey. Up to now, only the fluvial part of the Lower Seine River from Gennevillier to Poses has been considered. The Seine estuary has not been treated yet. The river is split into 4 reaches delimited by weirs and locks: between Chatou and Andresy (reach 1); between Andresy and Mericourt (reach 2); between Mericourt and Notre Dame La Garenne (reach 3); between Notre Dame La Garenne and Poses (reach 4).

On each fluvial reach, hydraulic models have been built on Telemac 2d (www.opentelemac.org) which solves the Saint-Venant equations using the finite-element method on unstructured grid [Hervouet, 2007]. Mesh size comprises within 60 000 to 120 000 nodes according to the reach length and the numbers of isle inside the reach. Distance between the mesh nodes varies between 3 m (typically in

ship locks) and 12.5 m (typically in the middle of the reach). For each reach, measured discharge is imposed at the upstream boundaries and measured water level is set for the downstream boundary. Friction coefficient is calibrated using measured water level at the upstream boundary.

The data used for this model is the December 2012 river freshet. The average discharge for Seine River between 2008 and 2015 is 480 m³/s. In December 2012, the river freshet started with low discharge (< 200 m³/s) during the first few days, then a first increase in discharge was observed (up to 500 m³/s) and a final surge in discharge (up to 950 - 1000 m³/s) occurred near the end of the event. Therefore, this event allows to simulate Seine river hydrodynamic conditions for three characteristic discharges (200, 500 and 900 200 m³/s). From these 2D hydraulic models, values of the water depth and flow velocities are extracted along the vessel path for different flowrate values.

3.4 Operating conditions

The itinerary on which the ship speed is optimized is characterized by a set of parameters called operating condition. These parameters are the channel width W, the water depth H and the current velocity U and are required in order to calculate the ship resistance with the model described in section 3.1. From 2D hydraulic models, water depth H, current velocity U and river width W are extracted every 10 m on the vessel trajectory. The itinerary is then approximated by n legs of length $li = 10\,m$ and characterized by the parameters $(H_i; U_i; W_i)_{1 \leq i \leq n}$. This itinerary is then further simplified for the optimization process by merging the n fine legs into N coarser legs LCi of length L_i, by using the Piecewise Aggregate Approximation technique (Keogh et al., 2001).

If $X = [x_1, \ldots, x_n]_{1 \leq i \leq n}$ is the list of parameters (x denotes either the water depth H, the current velocity U or the river width W) extracted every 10 m, the data $Y = [y_1, \ldots, y_n]_{1 \leq i \leq n}$ characterizing the N coarser legs is calculated as:

$$y_i = \frac{N}{n} \sum_{j=\frac{n}{N}(i-1)+1}^{\frac{n}{N}i} x_j \tag{7}$$

3.5 Optimization algorithm

The optimization algorithm minimizes the global fuel consumption for the itinerary by finding the optimal speed at which the ship should sail on each leg. The quantity of fuel FCi (kg) consumed by the ship on leg LCi of length Li (km) is given by:

$$FC_i = \dot{m}_{fi} \times \Delta T_i = SFC_i \times P_{Bi} \times \Delta T_i \tag{8}$$

where ΔT_i (h) is the time necessary for the ship to cover the distance L_i.

It is assumed that ship sails at constant speed V_i on leg LCi, therefore $\Delta T_i = L_i/V_i$. Equation (9) also gives $P_B = \frac{1}{\eta_H \times \eta_B \times \eta_S} P_E = \frac{R_{Ti} \times V_i}{\eta_H \times \eta_B \times \eta_S}$. As a result the quantity of fuel FC_i can be written:

$$FC_i = \frac{SFC_i \times R_{Ti} \times L_i}{\eta_H \times \eta_B \times \eta_S} \tag{10}$$

The total fuel consumption FC_T on the itinerary is then given by:

$$FC_T = \sum_{i=0}^{N} FC_i \tag{11}$$

The expression FC_T thus defined is a non-linear continuous function of variable $\boldsymbol{V} = (V_0, \ldots, V_N)$.

The formulation of the optimization problem can then be written as:

$$\begin{aligned} minimize \quad & FC_T(\mathbf{V}) \\ such\ that \quad & \sum_{i=0}^{N_C} \frac{L_i}{V_i} \leq T_{max} \\ & V_i > 0 \qquad\qquad i = 0, ..., n \end{aligned} \tag{12}$$

The first constraint set a maximum travel duration and the other constraints are only set to restrict the speed values to positive values. This optimization problem is a non-linear optimization problem with nonlinear constraints. Several methods are available to solve this type of optimization problem such as penalty function method, gradient projection method, feasible directions method and multiplier methods. However, these methods often perform better for linear constraints. For this reason, the optimization problem is reformulated as follows:

$$\begin{aligned} minimize \quad & FC_T^*(\mathbf{X}) \\ such\ that \quad & \sum_{i=0}^{N_C} L_i \times X_i \leq T_{max} \\ & X_i > 0 \qquad\qquad i = 0, ..., n \end{aligned} \tag{13}$$

where $X = \frac{1}{V} = \left(\frac{1}{V_0}, ..., \frac{1}{V_N}\right)$ and $FC_T^*(X) = FC_T\left(\frac{1}{X}\right) = FC_T(V)$. With this formulation, the problem is now a non-linear optimization problem with linear constraints in X.

4. **Application to a 135 m long vessel sailing on the Lower Seine River**

In the following sections, more details are provided on the results of the surrogate model for the ship resistance and on the optimization techniques. Then the speed optimization is applied to a 135 m long vessel on the Lower Seine River.
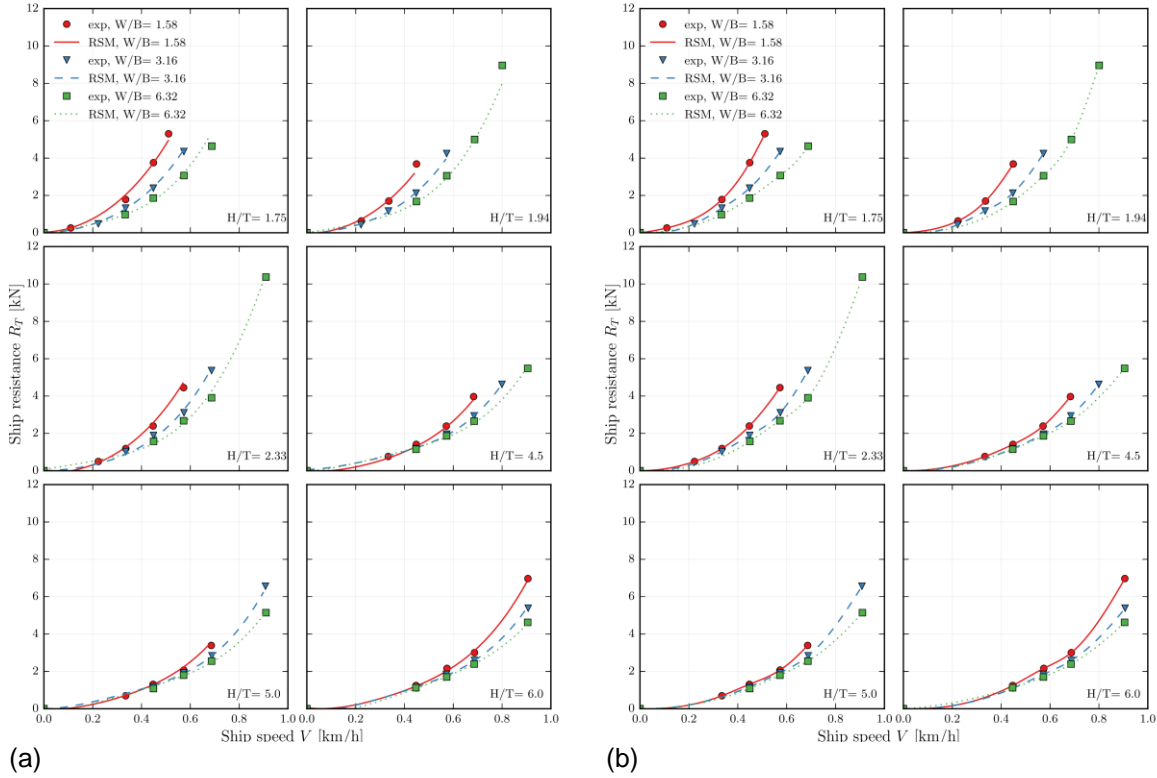
4.1 Surrogate model for ship resistance

Five different approaches have been tested: polynomial regression (PR), moving least square (MLS), Kriging, support vector regression (SVR) and radial basis functions (RBF). For these five methods, the surrogate model results have been compared to the Anast experimental results and the RMS has been calculated for each method. The RMS results are presented in Table 2:

Method	RMS
PR	0.2
MLS	0.04
Kriging	0.03
SVR	0.04
RBF	0

**Table 2 RMS values obtained for the 5 tested methods**

The mean square error calculated for the four tested methods showed that overall; MLS, Kriging, SVR and RBF methods give more accurate predictions than the PR method. It should also be mentioned that the RMS value for the RBF method is equal to 0 because this method in an interpolating method. Figure 5 illustrates the comparison between the experimental data (markers) and the surrogate models (lines) for the Kriging and RBF methods.

(a)   (b)

Figure 5: Comparison between experimental data and surrogate model output for (a) Kriging and (b) RBF methods

Figure 5 shows that both methods give accurate predictions for ship resistance. However, the evolution of the ship resistance curves is smoother in the case of the Kriging method than in the case of the RBF method.

Figure 6 shows the iso-contours of ship resistance in function of W/B and H/T at four different ship speeds (V=0.2, 0.4, 0.6 and 0.8 m/s) calculated with the Kriging and RBF method.
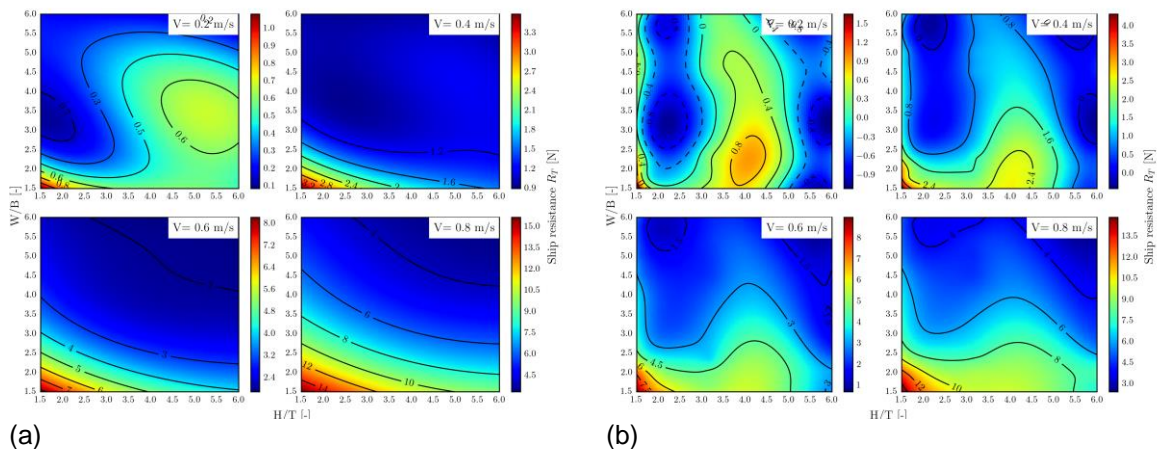
(a)   (b)

Figure 6 Iso-contours of ship resistance in function of W/B and H/T ratios at V=0.2,0.4, 0.6 and 0.8 m/s calculated with the (a) Kriging and (b) RBF methods

Figure 6 shows that the iso-contours of ship resistance obtained with RBF method are fairly irregular and this behavior does not represent a physical evolution of the ship resistance. The same

observations were made for the SVR method as well. However, the iso-contours of ship resistance calculated with the MLS and Kriging method showed a regular evolution, as illustrated in Figure 6 (a). Therefore, the MLS and Kriging methods are more adapted for this surrogate model. However, the MLS method is computationally more expensive than the Kriging method because the approximation coefficients have to be calculated for each prediction. The optimization process needing many function evaluations, the Kriging method is chosen for this surrogate model as it is computationally quicker than the MLS method.

4.2 Comparison of the optimization techniques

The four optimization techniques have been tested with a ship sailing upstream on Reach 1 for a discharge of 200 m³/s. 50 random uniformly distributed samples for initial speed distribution have been generated in the bounded region defined by the optimization problem (see Equation 12). This random sampling is based on the Billiard Walk algorithm [Gryazina and Polyak, 2014]. Each optimization technique has been run on this random sample and the average converging time to the solution is calculated. Table 3 shows the average number of iteration $Niter$, the average calculation time, the average total fuel consumption FC_T and its standard deviation σ_{FC} calculated for each method over the 50 initial speed samples.

Method	Niter [-]	Time [s]	$\mathbf{FC_T}$ [kg]	$\sigma_{\mathbf{FC}}$ [kg]
PM	14.0	18.2	466.98	0.002
GPM	6.84	3.24	467.05	0.011
FDM	17.14	8.60	476.34	4.88
SLQP	100.54	33.34	467.80	1.28

Table 3: Comparison of the optimization algorithm performance

From Table 3 it can be seen that each method converges to the same optimum fuel consumption value ($FC_T \approx 467\ kg$) except for the Feasible Direction Method. The standard deviation calculated for FDM and SLSQP is also important which indicates a large spreading of the optimum values found around the mean. Figure 7 illustrates the convergence of the Penalty Method, Feasible Direction Method and Gradient Projection Method for the first point of the random sample.
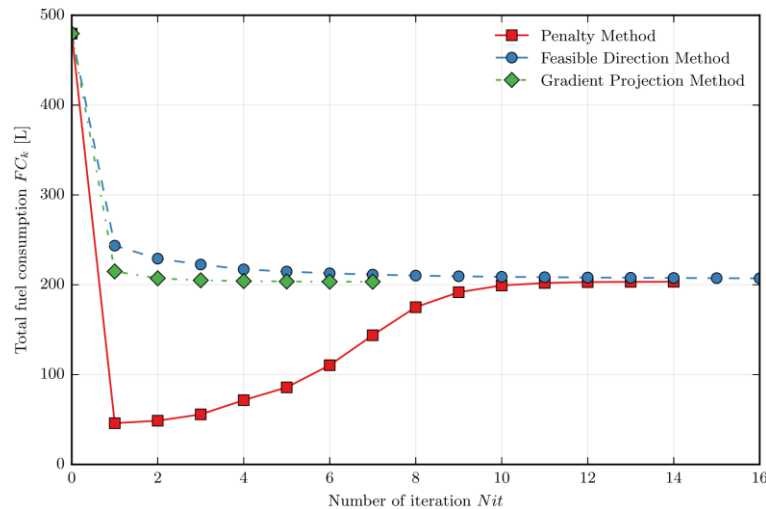

Figure 7 : Illustration of the convergence of Penalty Method, Feasible Direction Method and Gradient Projection Method for a random initial speed

Figure 7 shows that the Gradient Projection Method converges much faster (7 iterations) than the Penalty (14 iterations) and Feasible Direction Method (17 iterations). It can be seen that after the first iteration of the Penalty method, the solution is located outside of the feasible domain (the updated calculated speed solution is small which explains the low fuel consumption FC_T), therefore the penalty function is switched to exterior penalty function, and after a few iterations, the solution is brought back into the feasible domain and converges to the solution.

Table 3 also shows that the Penalty Method and Gradient Projection Method have lower standard deviation σ (better accuracy) and also converge faster than the SLSQP method. In average, the Gradient Projection Method is 6 times faster than the Penalty Method and shows good accuracy (low standard deviation). Overall, the Gradient Projection Method performs better than the three other optimization techniques tested for this problem. This method is particularly adapted for this problem because it projects the search direction into the subspace tangent to the active constraints which is where the solution lies. For these reasons, this method is used to solve the speed optimization problem.

4.3   Application of the speed optimization

Average AIS speed observed on each leg of the travel is used as initial speed profile for the optimization process. AIS data for a 135 m long vessel and covering three full months (November and December 2017 and January 2017) has been used for this study. To be as accurate as possible, for each AIS speed collected, its timestamp has been compared to the measured discharge at Chatou's dam and only AIS data corresponding to the studied discharges have been selected for the calculation of the mean speed on each leg. The discharge measured during this period does not exceed 700 m³/s. Therefore, speed optimization has been carried out for two river discharges: 200 m³/s and 500 m³/s. The maximum travel duration T_{max} is set as the travel time necessary for the ship to complete the itinerary with the mean AIS speed calculated on each leg. The ship draft T is 2 m corresponding to 3 layers of containers used for 80% of the travels for this ship.

Figure 8 and Figure 9 show the profile of (a) instant fuel consumption, (b) speed V and (c) water depth restriction H/T, in the case of AIS speed profile and optimized speed profile for a discharge $Q = 200\ m^3/s$ and a ship sailing upstream (Figure 8) and downstream (Figure 9).
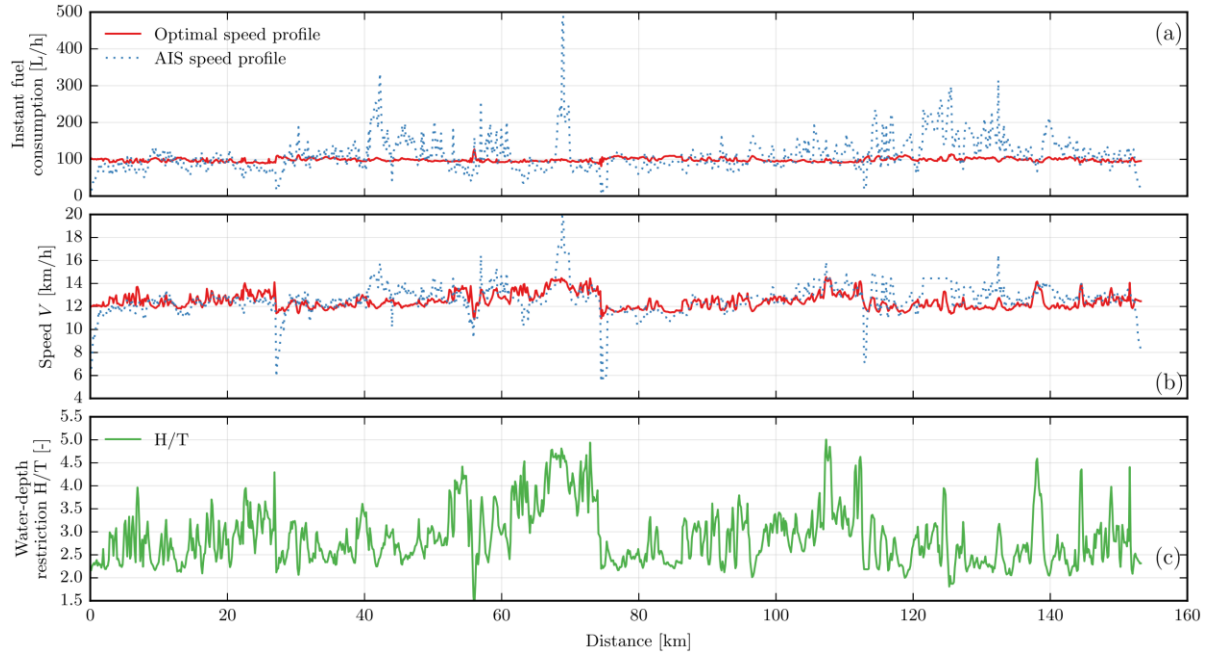
Figure 8: Profile of (a) instant fuel consumption,(b) speed V and (c) water depth restriction H/T for AIS and optimal speed ($Q = 200\ m^3/s$, upstream)

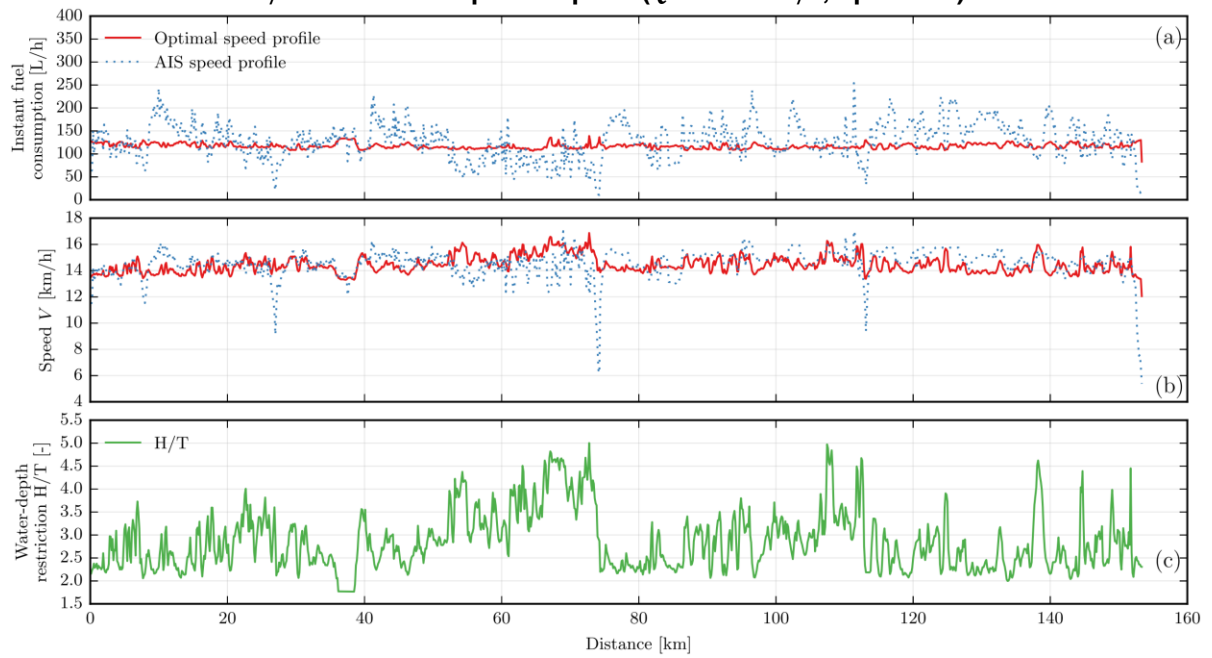**Figure 9: Profile of (a) instant fuel consumption,(b) speed V and (c) water depth restriction H/T for AIS and optimal speed ($Q = 200\ m^3/s$, downstream)**

Figure 8 and Figure 9 show that the speed profile observed with AIS data varies significantly over the travel length. The four low speed peaks observed at around 25, 75, 110 and 155 km correspond to a slow down of the ship when approaching a lock on the itinerary. Those two figures also show that the speed variation amplitude is less significant for the optimum speed profile than for the AIS speed profile.

For the optimal speed profiles, the instant consumption is relatively constant over the travel, which is not the case for the AIS speed profile. In those cases, the specific fuel consumption SFC remains nearly constant because the engine is operated at a regime where SFC curve is flat (see Figure 4). As a result, the engine power variation remains limited during the travel, which is in agreement with findings reported by Bons et al. [2014] that minimum fuel consumption is achieved on a waterway by operating in constant power.

The optimal speed profile and H/T profile also have the same shape (Figure 8 and Figure 9). The Seine being a wide river (around a hundred meters), water depth is the main parameter having an effect on the added resistance due to restriction. As a result, the ship will sail faster when restriction is less important and slow down for lower values of H/T.

Table 4 shows the average water depth $\overline{H}$, the average current velocity $\overline{Uc}$, the total fuel consumption for the AIS speed profile FC_{T0} and optimal speed profile FC_{Topt}, the mean fuel consumption (in L/km) for the AIS speed profile $\overline{FC_{T0}}$ and optimal speed profile $\overline{FC_{Topt}}$; and the fuel consumption reduction $FCR = (FC_{T0} - FC_{Topt})/FC_{T0} \times 100$ calculated for each of the 4 cases studied.

Q [m^3/s]	Dir. [-]	$\overline{\mathbf{H}}$ [m]	$\overline{Uc}$ [m/s]	FC$_{\mathbf{T0}}$ [L]	FC$_{\mathbf{Topt}}$ [L]	$\mathbf{\Delta}$FC$_{\mathbf{T}}$ [L]	$\overline{\mathbf{FC_{T0}}}$ [L/km]	$\overline{\mathbf{FC_{Topt}}}$ [L/km]	$\overline{\mathbf{FCR}}$ [%]
200	up	5.7	0.21	1327	1215	112	8.7	7.9	9.3
200	down	5.7	0.21	1335	1244	92	8.7	8.1	7.4
500	up	6.0	0.51	1974	1851	123	12.9	12.0	6.6
500	down	6.0	0.51	674	623	51	4.4	4.1	8.2

Table 4: Speed optimization results calculated for two discharges ($Q = 200 \ and \ 500 \ m^3/s$) and two sailing directions (upstream and downstream)

The fuel saving for a travel ΔFC_T vary between 51 L and 123 L with an average of 95 L (Table 4). The associated fuel consumption reduction FCR varies between 6.6% and 9.3% with an average of 7.9%. Finally, the average fuel consumption FC_T for the 4 tested cases is equal to 8.7 L/km for the AIS speed profile and 8.05 L/km for the optimum speed profile which is in agreement with the average fuel consumption of 8 L/km indicated by VNF [2006] for this type of vessel. The fuel consumption reduction FCR results presented in the table also show that the fuel savings obtained are more significant in the case of a ship sailing downstream. This difference could be explained by the fact that sailing against the flow limits the possible change in speed as it requires more power to increase the velocity of the ship.

4.4   Influence of trajectory and travel duration

With the aim of studying the influence of the lateral position of the ship in the channel, the previous simulation is compared with the results obtained when the ship is sailing in the deepest part of the river. In the latter scenario, the turning circle of the vessel is not taken into account and choosing the deepest part of the river occasionally create discontinuities in the trajectory. Figure 9 shows (a) the instant consumption, (b) the speed profile and (c) water depth restriction ratio H/T profile against the distance for the two scenarios.
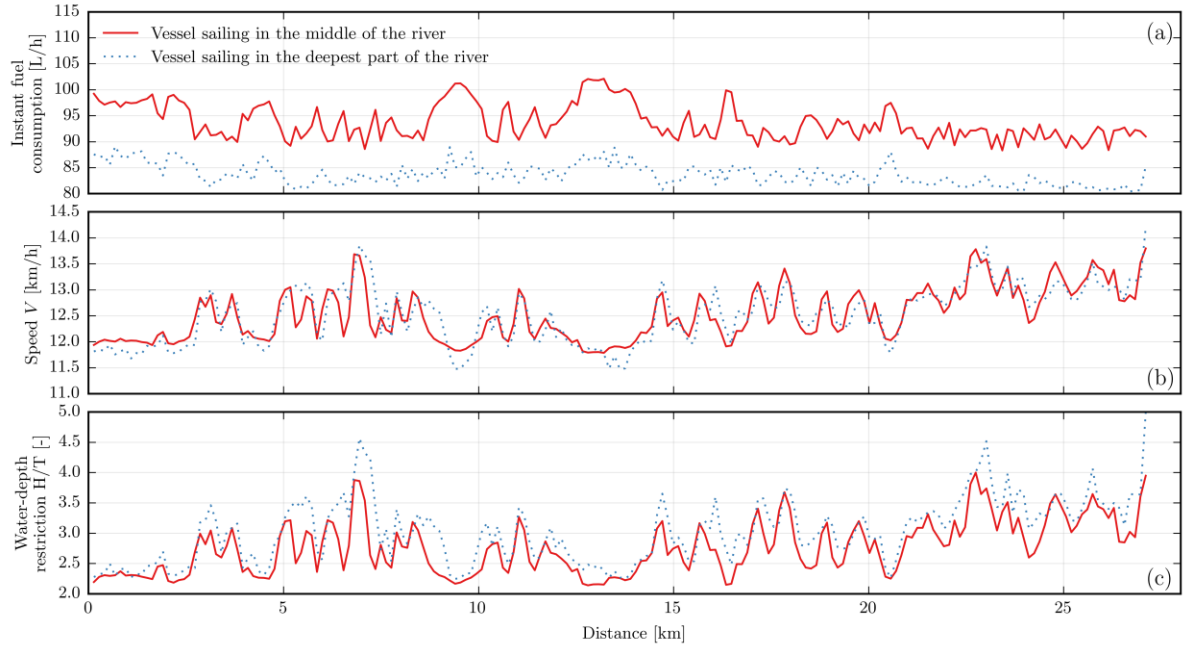
Figure 10: Profile of (a) instant fuel consumption, (b) speed V and (c) water depth restriction H/T for the vessel sailing in the middle and in the deepest part of the river (ship sailing upstream on Reach one for a discharge of 200 m³/s)

Figure 10 shows that the water depth profile in the case of a ship sailing in the middle and in the deepest part of the river have the same shape; however, the water depth restriction is less important for the ship sailing in the deepest part of the waterway. Both speed profiles also show the same pattern but the ship navigating in the deepest part of the river tends to go faster when the restriction is low and slower when it is important. As a result, the instant consumption is clearly lower in the case of the ship sailing at maximum depth. The main reason for that is that the added force due to water depth restriction is less important when the ship sails in the deepest part of the river. In the case of the ship sailing at maximum water depth, the total consumption obtained is FCTopt = 171:67kg for the optimal speed profile. The comparison with the consumption obtained for the first scenario gives a 9% reduction of the total fuel consumption. Although this reduction could be less important when taking turning circle into account, this result indicates choosing the optimal track can also lead to additional fuel savings. Theoretically, this track could be determined with up to date bathymetry data of Seine river bottom, but other factors also have to be taken into account such as the continuity of the trajectory and locally specific navigation rules.

The influence of travel duration on the optimal fuel consumption has been studied by running several simulations in which the maximum travel duration Tmax is increased, from 2h to 3h30. Figure 10 presents the evolution of the optimal fuel consumption FCT and the fuel consumption reduction defined by $FC_{Red} = \frac{FC_T(2h) - FC_T(T_{max})}{FC_T(2h)}$ against the máximum travel duration T_{max}.

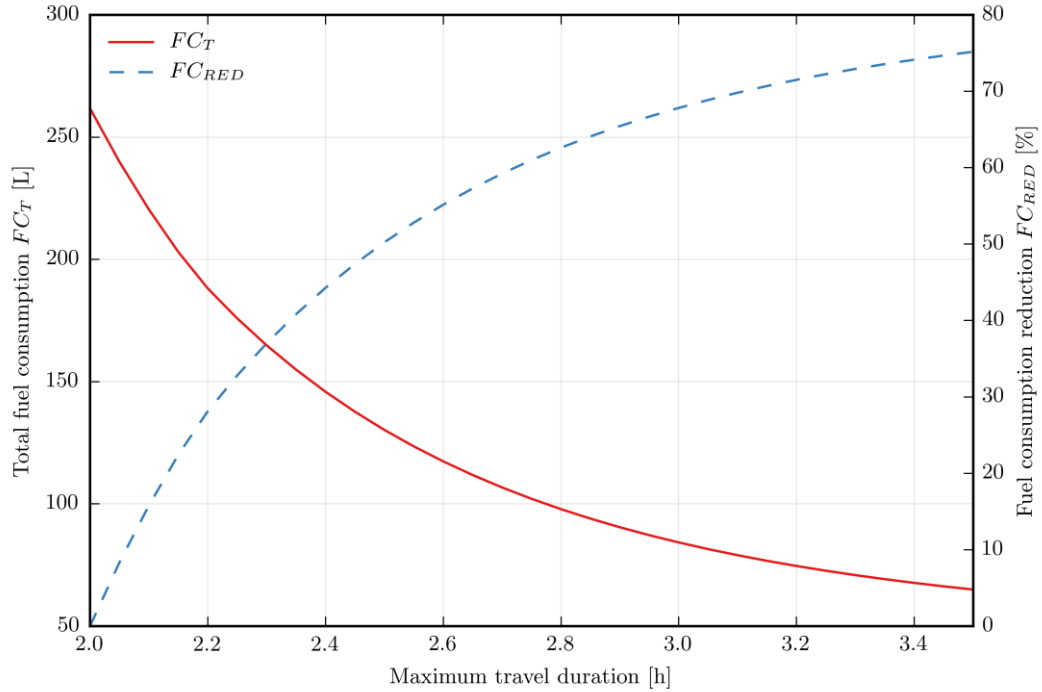**Figure 11: Evolution of total fuel consumption FCT and fuel consumption reduction FCRED against the maximum travel duration Tmax (ship sailing upstream on Reach one for a discharge of 200 m3/s)**

The fuel consumption decreases sharply for a travel duration between 2h and 2.5h and at a steadier rate afterwards (Fig 10). The main reason for this evolution is that the thrust power necessary to maintain a ship at a constant speed V is roughly proportional to V^3. Therefore, increasing the maximum travel duration allows to reduce the average speed; and the fuel consumption, linked to the thrust power, decreases in an exponential manner. For instance, a 12 minutes travel time increase, from 2h to 2h12, leads to a 26% fuel consumption decrease. This fact highlights another important aspect of fuel consumption optimization: including real time information in the optimization process can lead to additional fuel savings. For instance, knowing in advance that an approaching lock is unavailable due to maintenance or ship queue can be used to reduce the sailing speed in order to avoid waiting at the lock and make fuel savings.

5. **Conclusions and perspective**

EcoNav and its modules have been described in this paper and applied to a real case study. This model is based on an optimization algorithm minimizing the fuel consumption by finding the optimal speed profile for a given itinerary (operating conditions) under specified constraints (maximum travel duration). The fuel consumption is evaluated with a specific fuel consumption empirical model developed by Hidouche et al [2015] and a ship resistance surrogate model based on ship resistance experimental results from Anast towing tank. The operating conditions used by EcoNav (channel width, water depth and current velocity) are calculated by using a 2D hydraulic model (Telemac2D). Several methods for the surrogate model and the optimization process were tested and allowed to select the most appropriate (in terms of accuracy and speed) for EcoNav. EcoNav has been applied to study the itinerary of the self-propelled ship Oural on river Seine, between the locks of Chatou and Poses. The comparison between the optimum fuel consumption and the mean AIS observed speed on each leg of the itinerary, showed an average calculated fuel savings of 7.9 %. The average calculated fuel consumptions on this itinerary are in agreement with the results reported in VNF [2006]. The comparison of optimal fuel consumption obtained in the case of a ship sailing in the middle or in the deepest part of the waterway demonstrated that significant fuel savings can be expected by optimizing the vessels trajectory. Finally, it was shown that additional fuel consumption reduction can be realized by extending the duration of the travel. The latter solution could be used in case of lock unavailability or heavy traffic and would necessitate including real time information in the optimizing process. Altogether, this paper presented three ways of reducing fuel consumption: optimizing the speed and trajectory of a vessel and including real time information in the optimization process. The speed optimization model presented in this article is still at an early stage design and needs further improvement and validation. Several limitations to this model can be listed:

- the change in the ship speed is instantaneous and the acceleration/deceleration is not taken into account nor its impact on fuel consumption;

- the trajectory is linearised, as a result its curvature and impact on fuel consumption is neglected;

- wind effect on ship resistance and fuel consumption is not taken into account;

- the hydrodynamic model cannot currently simulate a sea tide and therefore EcoNav cannot be used in intertidal area;

- the ship consumption model needs further validation.

This model could be improved by taking into account the acceleration/deceleration of the ship in the fuel consumption model and the optimization process, and including the effects of the trajectory curvature in the model (rudder effects for instance). Existing empirical models for air resistance calculation could also be used to take the effect of wind into account in the fuel consumption model. The accuracy of the propulsion modelling could also be improved by using existing empirical models to calculate the various propulsion efficiencies. A project is currently ongoing to instrumentalize the 135 m self propelled ship Bosphore, in collaboration with Compagnie Fluviale de Transport, in order to realize a broad range of in situ measurement (fuel consumption, engines rpm, ship's speed and position,...) over the span of one year. Data recorded from this project will help improve and validate the ship fuel consumption model. Cerema is also involved in Seine RIS (River Information Service) and will work on the development of three modules: ETA prediction for inland ships, optimization of waiting times in river locks and estuary hydrodynamic model for the prediction of bridge clearance. The feedbacks from this project can contribute to include a sea tide effect and real time traffic information into EcoNav. When EcoNav has reached a higher maturity level, a prototype could be built and tested on a ship in situ.

References

Agence de l'Environnement et de la Maitrise de l'Energie (2006). Transports combinés rail-route, fleuve-route et mer-route : tableau de bord national. Technical report.

Bons, A., Molenmaker, K., and van Wirdum, M. (2014). Economyplanner; optimal use of inland waterways. In European Inland Waterway Navigation Conference, Budapest, 10th–12th September.

Federal German Water and Shipping Administration (2007). Economical and ecological comparison of transport modes: road, railways, inland waterways. Technical report.

Foeth, E. (2008). Decreasing frictional resistance by air lubrication. In 20th International HISWA Symposium on Yacht Design and Yacht Construction, Amsterdam, The Netherlands.

Forrester, A. I. and Keane, A. J. (2009). Recent advances in surrogate-based optimization. Progress in Aerospace Sciences, 45(1):50–79.

Geerts, S., Verwerft, B., Vantorre, M., and Van Rompuy, F. (2010). Improving the efficiency of small inland vessels. In Proc., 7th European Inland Waterway Navigation Conference. Budapest University of Technology and Economics, Budapest, Hungary.

Georgakaki, A. and Sorenson, S. (2004). Report on collected data and resulting methodology for inland shipping. Lyngby, Denmark, Technical University of Denmark.

Gryazina, E. and Polyak, B. (2014). Random sampling: Billiard walk algorithm. European Journal of Operational Research, 238(2):497–504.

Hidouche, S., Guitteyn, M.-H., Linde, F., and Sergent, P. (2015). Ships propulsion : estimation of specific fuel consumption based on power load factor ratio. In Proc., Hydrodynamics and simulation applied to inland waterways and port approaches. SHF, Société hydrotechnique de France.

Jastrzebski, T., Sekulski, Z., Taczala, M., Graczyk, T., Banasiak, W., and Zurawski, T. (2003). A concept of the inland waterway barge base on the i-corer steel panel. In European Inland Waterway Navigation Conf., Gyor.

Landweber, L. (1939). Tests of a model in restricted channels. EMB Report 460.

Linde, F., Ouahsine, A., Huybrechts, N., and Sergent, P. (2016). Three-dimensional numerical simulation of ship resistance in restricted waterways: Effect of ship sinkage and channel restriction. Journal of Waterway, Port, Coastal, and Ocean Engineering, 143(1):06016003.

MAN (2011). Basic principles of ship propulsion.

MoVe IT! FP7 European project (2012). Deliverable 1.1 state of the art. Technical report.

Noury, P., Hayman, B., McGeorge, D., and Weitzenbock, J. (2002). Lightweight construction for advanced shipbuilding–recent development. Det Norske Veritas, Norway.

Psaraftis, H. N. and Kontovas, C. A. (2014). Ship speed optimization: Concepts, models and combined speed-routing scenarios. Transportation Research Part C: Emerging Technologies, 44:52–69.

Queipo, N. V., Haftka, R. T., Shyy, W., Goel, T., Vaidyanathan, R., and Tucker, P. K. (2005). Surrogate-based analysis and optimization. Progress in aerospace sciences, 41(1):1–28.

Radojčić, D. (2009). Environmentally friendly inland waterway ship design for the danube river. World Wide Fund for Nature International Danube-Carpathian Programme (WWF-DCP).

Rohács, J. and Simongati, G. (2007). The role of inland waterway navigation in a sustainable transport system. Transport, 22(3):148–153.

Rosen, J. B. (1960). The gradient projection method for nonlinear programming. part i. linear constraints. Journal of the Society for Industrial and Applied Mathematics, 8(1):181–217.

Rotteveel, E., Hekkenberg, R., and Liu, J. (2014). Design guidelines and empirical evaluation tools for inland ships. In Proc., 7th European Inland Waterway Navigation Conference. Budapest University of Technology and Economics, Budapest, Hungary.

Schlichting, O. (1934). Ship resistance in water of limited depth-resistance of sea–going vessels in shallow water. Jahrbuch der STG, 35:127–148.

Simpson, T. W., Toropov, V., Balabanov, V., and Viana, F. A. (2008). Design and analysis of computer experiments in multidisciplinary design optimization: a review of how far we have come or not. In 12th AIAA/ISSMO multidisciplinary analysis and optimization conference, volume 5, pages 10–12.

Stenzel, V., Wilke, Y., and Hage, W. (2011). Drag-reducing paints for the reduction of fuel consumption in aviation and shipping. Progress in Organic Coatings,70(4):224–229.

VNF (2006). Etude sur le niveau de consommation de carburant des unités fluviales françaises. Technical report.

Zöllner J. (2003) Vortriebstechnische Entwicklungen in der Binnenschifffahrt. 24. Duisburger Kolloquium Schiffstechnik/Meerestechnik. Universität Duisburg-Essen Institut für Schiffstechnik und Transportsysteme. 15–16 May, pp 134.